

trans-Polyacetylene on Sodium and Cesium Mordenites: A Resonance Raman Spectroscopic Study

Andrew R. Lewis, Graeme J. Millar, Ralph P. Cooney,* and Graham A. Bowmaker

Department of Chemistry, University of Auckland, Private Bag 92019, Auckland, New Zealand

Received May 12, 1993. Revised Manuscript Received July 23, 1993*

Sodium and cesium mordenite (denoted NaM and CsM, respectively) were investigated as potential catalysts for the synthesis of polyacetylene ((CH)_x). Both were successful in initiating polymerization of purified gaseous acetylene at room temperature as evidenced by Raman spectroscopic studies. The polyacetylene synthesised in this way exhibited resonance enhancement of the polyene skeletal vibrations. *trans*-Polyacetylene, but no *cis*-(CH)_x, was detected. As no apparent coloration of the NaM and CsM substrates accompanied the formation of *trans*-(CH)_x it was concluded that only small quantities of the polymer were present. The number of conjugated double bonds was estimated from the frequencies of the Raman active C-C and C=C stretching vibrations, and it was shown that the *trans*-(CH)_x formed on CsM has a distribution of conjugation lengths ranging from less than 6 to at least 30 double bonds. The polyacetylene formed on NaM was significantly shorter and was produced in lower yields than that synthesized on CsM. "Sliced" resonance excitation profiles of polyacetylene formed on CsM were obtained using nearly 40 different excitation wavelengths and these confirmed that the adsorbed *trans*-(CH)_x was composed of segments having a distribution of conjugated lengths. The architecture of the mordenite pore system permitted only a single polymer molecule per channel, thereby preventing cross-linking. Raman spectroscopic studies of the effects of exposure to air revealed that progressive oxidative degradation occurred with a reduction in the number of conjugated double bonds.

Introduction

Polyacetylene (denoted (CH)_x) has attracted much attention on account of its ability to act as an electronic conductor when oxidized or reduced (the process of oxidation or reduction being referred to as "doping").¹ The properties of polyacetylene are highly dependent on both the synthesis conditions and the postsynthesis treatment.¹ Although polyacetylene exhibits high electrical conductivities in the doped state, its utility as a conducting polymer is limited by its instability in air. Polyacetylene has been synthesised using a variety of methods. Free-standing polyacetylene films (i.e., bulk (CH)_x) are generally prepared from acetylene gas using a Ziegler-Natta type catalyst (e.g., titanium tetrabutoxide triethylaluminum (Ti(OC₄H₉)₄-Al(C₂H₅)₃) with pure *cis*-(CH)_x as the product if the reaction is carried out below 195 K. The pure *trans* isomer is obtained for synthesis temperatures above 373 K, with a mixture of both isomers produced at intermediate temperatures.¹ It has been demonstrated that the *trans*-(CH)_x present in *cis*-(CH)_x films arises from thermal isomerization of the *cis* isomer. Since the molecular weight of polyolefins produced in Ziegler-Natta polymerizations decreases with increasing temperature,¹ the method of choice for obtaining good quality *trans*-(CH)_x is heating of the pure *cis* film at temperatures above 463 K.

trans-Polyacetylene has also been produced by acetylene contact with oxides including Al₂O₃,^{2,3} TiO₂,⁴ and alumina-

supported rhodium.⁵ Several groups have reported the preparation of various polymers within the channels of certain zeolites.^{2,6-9} Encapsulation of polymers within the channels of a zeolite which prohibits cross-linking between adjacent oligomers could aid understanding of the physical properties of conducting polymers, and such materials may even exhibit unique properties due to the regular, crystalline lattice in which the polymers are formed.⁶⁻⁹

The quality of polyacetylene is directly related to both the molecular weight and the average length of sequences of uninterrupted conjugated double bonds (N_{C=C}) with a good-quality sample having a high molecular weight and a large N_{C=C} value. Resonance Raman spectroscopy of polyacetylene has provided¹⁰ a method of determining the length of conjugation in the polymer backbones, and this has revealed that there is a distribution of segment lengths.^{11,12} The large number of resonance Raman studies that have been reported have also yielded direct information as to the nature of the excited electronic state and these have been summarized by various workers.^{1,13,14}

(3) Heaviside, H.; Hendra, P. J.; Tsai, P.; Cooney, R. P. *J. Chem. Soc., Faraday Trans. 1* 1978, 74, 2542.

(4) Rives-Arnaud, V.; Sheppard, N. *J. Chem. Soc., Faraday Trans. 1* 1980, 76, 394.

(5) Parker, W. L.; Siedle, A. R.; Hexter, R. M. *J. Am. Chem. Soc.* 1985, 107, 264.

(6) Dutta, P. K.; Puri, M. *J. Catal.* 1988, 111, 453.

(7) Bein, T.; Enzel, P. *Mol. Cryst. Liq. Cryst.* 1990, 831, 315.

(8) Bein, T.; Enzel, P. *Angew. Chem., Int. Ed. Engl.* 1989, 28, 1326.

(9) Bein, T.; Enzel, P. *J. Chem. Soc., Chem. Commun.* 1989, 1326.

(10) Harada, I.; Furukawa, Y.; Arakawa, T.; Takeuchi, H.; Shirakawa, H. *Mol. Cryst. Liq. Cryst.* 1985, 117, 335.

(11) Brivio, G. P.; Mulazzi, E. *Phys. Rev. B* 1984, 30, 876.

(12) Tarr, A. W.; Siebrand, W. *J. Raman Spectrosc.* 1989, 20, 209.

(13) Tanaka, J.; Tanaka, M. In *Handbook of Conducting Polymers*; Skotheim, T. A., Ed.; Marcel Dekker Inc.: New York, 1986; Vol. 2, Chapter 35.

* Abstract published in *Advance ACS Abstracts*, September 1, 1993.

(1) Chien, J. C. W. *Polyacetylene; Chemistry, Physics, and Material Science*; Academic Press: New York, 1984.

(2) Tsai, P.; Cooney, R. P.; Heaviside, H.; Hendra, P. *J. Chem. Phys. Lett.* 1978, 59, 510.

In the present paper we report the results of a resonance Raman study of the products of polymerization of acetylene on the zeolite mordenite, which was chosen for its structural properties, principally the large (0.60 nm × 0.70 nm) linear channels. Like all zeolites, the properties of mordenite are influenced strongly by pore structure, the stoichiometry of the aluminosilicate framework, and the location, number, and type of cations present.¹⁵

Two forms of mordenite were chosen, these being the sodium and cesium exchanged forms (NaM and CsM respectively). These forms were chosen to elucidate the mechanism of acetylene polymerization. Cesium-exchanged X faujasite is known to activate and polymerize acetylene, but only monomeric acetylene is detected on sodium zeolite X.²

Experimental Section

The cesium-exchanged form of mordenite was prepared from parent NaM using conventional ion-exchange techniques. The parent sodium mordenite was Toyo Soda Manufacturing Co. TSZ NAA 620 (surface area 400 m² g⁻¹, density 0.35 g cm⁻³ and quoted oxide weight percentages: SiO₂ 81.6%, Al₂O₃ 9.2%, and Na₂O 5.5%) and was a slightly dealuminated form, having a silicon-to-aluminum ratio of 7.4 and unit cell composition Na_{5.4}Al_{5.4}Si₄₀O₉₆. Samples of parent NaM (ca. 3 g) were stirred continuously with an aqueous solution of 0.5 mol L⁻¹ cesium chloride (BDH, AnalaR grade) for 6 h at room temperature. The zeolite was then allowed to settle and the supernatant liquid decanted. A fresh amount of the appropriate aqueous chloride solution was added, and the treatment repeated. After five such treatments the exchanged mordenite was filtered off and thoroughly washed with Milli-Q water and then dried overnight at 393 K. Finally, the dried product was ground into a fine powder and stored in a desiccator. No color change was observed after exchange; the CsM formed retained the off-white color of NaM.

The sodium and cesium contents in the exchanged mordenite were determined by a method involving back exchange of sodium and cesium by silver followed by analysis of the exchange solution for sodium and cesium by atomic absorption spectroscopy. The calculated sodium content for NaM was in excellent agreement with the known unit cell composition of NaM (Na_{5.4}Al_{5.4}Si₄₀O₉₆). For CsM, some residual sodium was also detected and the calculated composition obtained was Cs_{4.8}Na_{0.8}Al_{5.4}Si₄₀O₉₆ indicating about 86% exchange of cesium for sodium.

X-ray diffraction (XRD) was used to check that the structural integrity of the mordenite was maintained after ion exchange or activation. Comparison of the XRD patterns obtained for NaM and for CsM before and after activation with the simulated diffraction pattern calculated for idealised sodium mordenite¹⁶ showed virtually identical peak positions in all cases, indicating that the structural integrity of the mordenite was maintained after ion exchange, and also upon heating at 773 K in oxygen for 12 h in the case of CsM.

Activation of the samples was achieved using the following procedure. First, mordenite powders were pressed into self-supporting wafers and then placed in a Pyrex reaction cell which was attached to a conventional vacuum line. After initial evacuation at ambient temperature the sample was heated to 393 K for 15 min in order to remove adsorbed water. Subsequently the temperature was raised to 773 K under a dynamic vacuum whereupon 90 kPa of oxygen (NZIG, Industrial grade) was admitted to the cell. The catalyst was then calcined at 773 K for 12 h by which time any organic impurities were assumed to have been combusted. Finally the sample was evacuated at 773 K for 15 min and then allowed to cool to ambient temperature under dynamic vacuum.

Acetylene gas (NZIG, Industrial grade) which had previously been purified by passage through a three-stage system consisting of a dry ice-acetone cold-trap (195 K), a concentrated sulfuric acid bubbler, and a column of dry potassium hydroxide pellets^{2,3} was then admitted into the cell at room temperature. This was done either as a series of small (0.5–5 kPa) increments or as a single dose to give a final pressure of ca. 80 kPa. The cell was then sealed off from the vacuum manifold or, in some cases, evacuated again after the mordenite had been in contact with acetylene for 5 min.

All Raman spectra of the samples were recorded at room temperature using either a Jobin-Yvon U1000 or Anaspec-Cary 81 Raman spectrometer. Several spectral regions were studied including general, wide scans over the range 200–2000 and 2100–3050 cm⁻¹ (with 1.0-cm⁻¹ sampling increment and 1.0-s integration time) or the higher data point density scans over the regions of 1000–1250 and 1400–1650 cm⁻¹ (0.5-cm⁻¹ increments, 2.0 s). Resolution was varied from 2 to 5 cm⁻¹.

Nearly 40 different excitation wavelengths ranging from 457.9 to 676.4 nm were used. These were provided by an argon ion laser (457.9–514.5 nm), a krypton ion laser (647.1 and 676.4 nm), and an argon ion pumped tuneable dye laser using rhodamine 6G dye which enabled wavelengths in the range 570–620 nm to be obtained. The wavelength of a given dye laser line was accurately determined by scanning the exciting line. The pyrex Raman cell containing the sample wafer was held vertically with the surface of the wafer at an angle of approximately 45° with respect to the incident laser light. The scattered radiation was collected at 90° by the spectrometer.

Spectra were recorded at incident laser powers ranging from 10 to 200 mW after various periods of acetylene contact (ranging from less than 1 h to 26 days), and in some cases after the acetylene had been removed by evacuation at room temperature. In a further series of experiments the effect of air exposure was followed by recording spectra of the sample after exposure to air for periods of between 1 h and 5 months. For these experiments the sample wafer was placed on a glass slide and Raman spectra were recorded using the Raman microscope attachment on the JY-U1000 employing 180° backscattering geometry. Both the 10 and 40 times magnification lenses were utilized with an incident laser power of 70 mW.

Results and Discussion

Other groups^{2–4,17} have reported a distinct, often rapid color change of the substrate during acetylene contact with various activated zeolites and oxides, which was attributed to formation of the conjugated polyene *trans*-(CH)_x. No visible coloration of the activated NaM or CsM samples was observed even after lengthy (26 days) periods of exposure to acetylene gas at room temperature, which suggested that only a small quantity of *trans*-polyacetylene was formed. However, due to resonance enhancement of certain modes, good quality Raman spectra could be obtained.

Representative Raman spectra recorded with 514.5-nm excitation over the region 200–2000 cm⁻¹ for samples of NaM and CsM in contact with 80 kPa of acetylene at room temperature are shown in Figure 1. The lattice modes (O–Si(Al)–O bending) of the mordenite substrates manifest themselves as the bands at ca. 390 and 460 cm⁻¹ in these spectra.¹⁸ These bands show small but significant shifts between the cesium and sodium ion forms, being observed at 393 and ca. 450 cm⁻¹ for CsM and 397 and ca. 465 cm⁻¹ for NaM. Preliminary Raman studies (using the 1974-cm⁻¹ band of gaseous acetylene as a reference) indicated that these modes exhibited normal Raman scattering across the range of excitation wavelengths used (457.9–676.4 nm), and because the ca. 390-cm⁻¹ band was

(14) Gussoni, M.; Castiglioni, C. Zerbi, G. *Adv. Spectrosc.* 1991, 19, 251.

(15) Mortier, W. J. *Compilation of Extra Framework Sites in Zeolites*; Butterworth and Co.: London, 1982.

(16) Ballmoss, R. V. *Collection of Simulated XRD Powder Diffraction Patterns for Zeolites*; Mobil Corp.

(17) Yates, D. J. C.; Lucchesi, P. J. *J. Chem. Phys.* 1961, 35, 243.

(18) Pechar, F.; Rykl, D. *Zeolites* 1983, 3, 329.

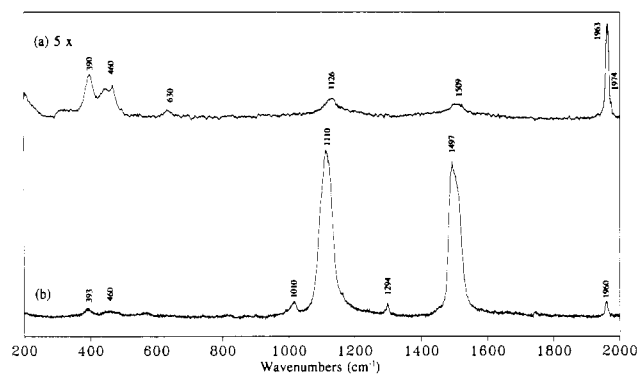


Figure 1. Resonance Raman spectrum of *trans*-(CH)_x formed by acetylene gas (273 K, 80 kPa) contact with (a) sodium and (b) cesium mordenite in the region 200–2000 cm⁻¹. Excited at 514.5 nm, laser power 200 mW, resolution 2.7 cm⁻¹, sampling increment 1.0 cm⁻¹.

generally better resolved it was utilized for normalizing the intensities of the other Raman bands within the same spectrum to correct for different incident laser powers.

Bands at ca. 1960, 1974, and 630 cm⁻¹ are completely removed upon evacuation of the cell for less than 5 min at room temperature and are assigned to monomeric acetylene. The weak, sharp band at 1974 cm⁻¹ is readily assigned to the ν_2 mode of gaseous acetylene.^{19,20} In agreement with the conclusions of several groups who have studied the adsorption of gaseous acetylene on various oxides and zeolites,^{2,3,21–28} the bands observed at 1963 and 1960 cm⁻¹ on NaM and CsM, respectively, are assigned to the ν_2 vibration of adsorbed monomeric acetylene interacting with the zeolitic cations (Na⁺ or Cs⁺) in a “side-on” fashion through its π -system. Similarly the very weak, broad band detected at ca. 630 cm⁻¹ may be assigned to the H—C≡C bending mode of monomeric acetylene adsorbed in a “side-on” manner.

Bands in the region 1000–1520 (Figure 1) and 2100–3050 cm⁻¹ (Figure 2) remained unchanged after evacuation of the sample cell, and these are assigned to adsorbed polyacetylene, as discussed below.

Spectra of Adsorbed Polyacetylene. The four bands in the region 1000–1520 cm⁻¹ are readily assigned to *trans*-polyacetylene (see Table I) adsorbed on the mordenites. The band assignments in the case of the CsM substrate are as follows: 1497 cm⁻¹ to the totally symmetric C=C stretching with considerable mixing of CH in-plane deformation (ν_1); 1294 cm⁻¹ to the C—C symmetric stretching vibration, (ν_2); 1110 cm⁻¹ to CH in-plane deformation with large C=C stretch contributions (ν_3) and 1010 cm⁻¹ to C-H out-of-plane wagging (ν_7). The 1509-, 1292-, 1126-, and 1011-cm⁻¹ bands observed after NaM was exposed to acetylene are similarly ascribed to the ν_1 ,

ν_2 , ν_3 , and ν_7 modes of adsorbed *trans*-(CH)_x, respectively. Comparison of these frequencies with those reported by Rives-Arnau and Sheppard⁴ for *trans*-(CH)_x on TiO₂ and by Tsai et al.² for polyacetylene on CsX which are given in Table I shows good agreement, in general, although there are quite large variations in the ν_1 and ν_3 frequencies between the different substrates but all fall within ranges reported for bulk *trans*-(CH)_x.¹

Bands are also observed in the region 2100–3050 cm⁻¹ (Figure 2), and these are readily assigned to combinations and overtones of the fundamental modes of adsorbed-*trans*-(CH)_x including $\nu_3 + \nu_7$, $2\nu_3$, $\nu_2 + \nu_3$, $\nu_1 + \nu_7$, $\nu_1 + \nu_3$ and $\nu_1 + \nu_2$. The combination mode $\nu_2 + \nu_7$ was only strong enough to be observed with blue excitation (457.9 and 488.0 nm). The broad double band observed at ca. 3000 cm⁻¹ is assigned to a Fermi resonance between the symmetric CH stretching mode, ν_8 (CH) and the first overtone of the ν_1 fundamental, $2\nu_1$ in agreement with Rives-Arnau and Sheppard.⁴ These assignments are summarized in Table I.

Figure 3 shows the spectra recorded with different excitation wavelengths in the 200–2000-cm⁻¹ region. These show that the positions, shapes, and relative intensities of the *trans*-(CH)_x Raman lines vary significantly with excitation frequency. These changes are most obvious in the ν_1 and ν_3 bands, which are shifted to lower frequencies with increasing excitation wavelength. Excitation-dependent band shifts were also observed for the overtone and combination modes in the 2100–3050-cm⁻¹ region. Tables II and III summarise the band frequencies observed with different excitation energies and their assignments for the 200–2000- and 2100–3050-cm⁻¹ regions respectively.

A detailed investigation of the Raman band dispersion was undertaken in order to obtain further information about the nature of the polymer formed under these conditions. The much lower intensity of the Raman spectra of the polymer recorded for samples of NaM relative to those for CsM prepared under identical conditions indicates that less polyacetylene was produced on the sodium form (i.e., NaM is not as good a polymerization catalyst as CsM). Consequently, detailed measurements of the Raman band dispersion were carried out for the cesium mordenite samples only.

Raman Band Dispersion. Band Shapes. Figure 4 shows typical Raman profiles obtained for the ν_1 mode of *trans*-(CH)_x adsorbed on CsM with 457.9-, 488.0-, 514.5-, 647.1-, and 676.4-nm excitation. The full band widths at half-peak maximum (fwhm) observed for these bands are listed in Table IV. As can be seen from Figures 3 and 4, the ν_1 and ν_3 bands did not show the double peak structure apparent in the Raman spectra of bulk *trans*-polyacetylene reported by several groups.^{32–35} In particular there was no strong, sharp low-frequency component which remained at constant position with variations in excitation energy, only a broad band which showed dispersion behavior

(19) Herzberg, G. *Infrared and Raman Spectra of Polyatomic Molecules*; Van Nostrand Reinhold: New York, 1945; pp 288–290.

(20) Dollish, F. R.; Fateley, W. G.; Benteley, F. F. *Characteristic Raman Frequencies of Organic Compounds*; John Wiley & Sons: New York, 1974; p 102.

(21) Tam, N. T.; Cooney, R. P.; Curthoys, G. *J. Chem. Soc., Faraday Trans. 1* 1976, 72, 2577.

(22) Tam, N. T.; Cooney, R. P.; Curthoys, G. *J. Chem. Soc., Faraday Trans. 1* 1976, 72, 2592.

(23) Bhasin, M. M.; Curran, C.; John, G. S. *J. Phys. Chem.* 1970, 74, 3973.

(24) Howard, J.; Robson, K.; Waddington, C.; Kadir, Z. A. *Zeolites* 1982, 2, 3.

(25) Riley, P. E.; Seff, K. *Inorg. Chem.* 1975, 14, 714.

(26) Amaro, A. A.; Seff, K. *J. Chem. Phys.* 1974, 77, 906.

(27) Howard, J.; Robson, K.; Waddington, C. *Zeolites* 1981, 1, 175.

(28) Howard, J.; Waddington, C. *Surf. Sci.* 1977, 68, 86.

(29) Lefrant, S.; Lichtmann, L. S.; Temkin, H.; Fitchen, D. B. *Solid State Commun.* 1979, 29, 191.

(30) Takeuchi, H.; Furukawa, Y.; Harada, I.; Shirakawa, H. *J. Chem. Phys.* 1986, 84, 2882.

(31) Takeuchi, H.; Arakawa, T.; Furukawa, Y.; Harada, I.; Shirakawa, H. *J. Mol. Struct.* 1987, 158, 179.

(32) Schügerl, F. B.; Kuzmany, H. *J. Chem. Phys.* 1981, 74, 953.

(33) Lichtmann, L. S.; Sarhangi, A.; Fitchen, D. B. *Chem. Scripta* 1981, 17, 149.

(34) Schen, M. A.; Chien, J. C. W.; Perrin, E.; Lefrant, S.; Mulazzi, E. *J. Chem. Phys.* 1988, 89, 7615.

(35) Mulazzi, E.; Brivio, G. P.; Faulques, E.; Lefrant, S. *Solid State Commun.* 1983, 46, 851.

Table I. Assignment of the Raman Bands of *trans*-polyacetylene

no. ^a	sym species ^b	assignment ^a	bulk film ^c	band position/cm ⁻¹			
				on CsM ^{d,e}	on NaM ^{d,e}	on CsX ^{e,f}	on TiO ₂ ^{e,g}
ν_5	B _u	in-plane longitudinal acoustic mode (LAM)	610 vw ^h	n.o.	n.o.	n.o.	n.o.
ν_8	B _g	C-H out-of-plane wagging ⁱ	878-884 w	n.o.	n.o.	n.o.	n.o.
ν_7	A _u ^j	C-H out-of-plane wagging ^k	1008-1016 s	1010 m	1011 vw	n.o.	1008 s
ν_3	A _g	C-H in-plane def with large C=C str contribution	1090-1130 vs	1110 vs	1126 m	1112 s	1108 vs
ν_2	A _g	C-C stretch	1292-1296 s	1294 w	1292 vw	n.o.	1294 m
ν_1	A _g	C=C sym str with considerable addition of C-H in-plane def	1470-1520 vs	1497 vs	1509 m	1503 s	1487 vs
$\nu_6(\text{CH})$	A _g	C-H sym str	2990 w	n.o.	n.o.	n.o.	2980 w ^l
		combination $\nu_3 + \nu_7$	2140 w ^{e,m}	n.o.	n.o.	n.o.	2092 w ⁿ
		overtone $2\nu_3$	2250 s ^{e,m}	2216 m	2250 w	2220 vw ^o	2196 s
		combination $\nu_2 + \nu_3$	2415 w ^{e,m}	2406 w	n.o.	n.o.	2381 vw
		combination $\nu_1 + \nu_7$	2520 w ^{e,m}	2504 w	n.o.	n.o.	2496 vw ⁿ
		combination $\nu_1 + \nu_3$	2630 s ^{e,m}	2604 m	2633 w	2600 vw ^o	2580 m
		combination $\nu_1 + \nu_2$	2800 w ^{e,m}	2790 w	n.o.	n.o.	2780 w
Fermi resonance $2\nu_1/\nu_3(\text{CH})$	3010 m ^{e,m}	2960/3001 m	2922 w	3010 vw ^o	2955/3000 m		

^a After refs 30 and 31. ^b For *trans*-(CH)_x of factor group C_{2h}. ^c From ref 1 (spectra recorded with range of excitation wavelengths). ^d This work. ^e Excited at 514.5 nm. ^f From ref 2. ^g From ref 4. ^h Not observed with visible light excitation. ⁱ Opposite direction at both ends of a CH=CH group. ^j Observed due to lowering of symmetry arising from polymer chain distortion. ^k Same direction at both ends of a CH=CH group. ^l Estimated. ^m Reported²⁹ for sample having $\nu_1 = 1507 \text{ cm}^{-1}$, $\nu_2 = 1290 \text{ cm}^{-1}$, $\nu_3 = 1126 \text{ cm}^{-1}$, and $\nu_7 = 1015 \text{ cm}^{-1}$. ⁿ Shoulder. ^o Broad; w = weak, m = medium, s = strong, v = very, n.o. = not observed.

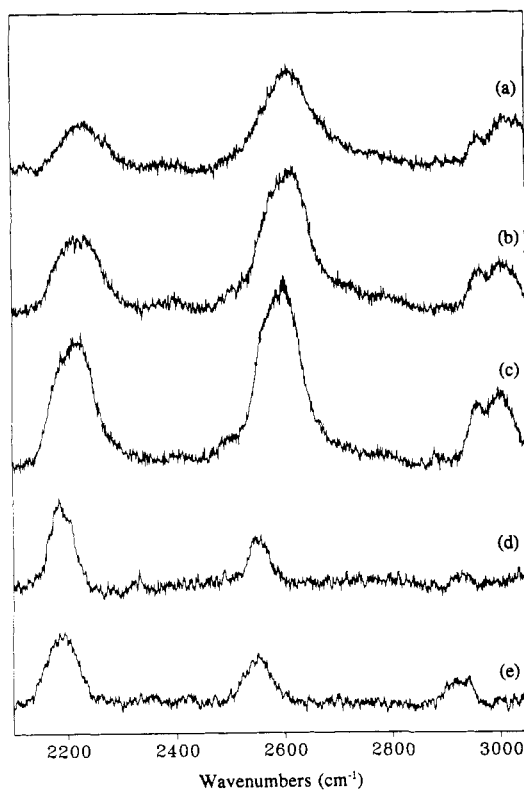


Figure 2. Raman spectrum of *trans*-(CH)_x on CsM in the region 2100-3050 cm⁻¹ showing overtone and combination bands. Excited at (a) 457.9, (b) 488.0, (c) 514.5, (d) 647.1, and (e) 676.4 nm.

similar to that of the so-called "satellite" peaks in these spectra. The experimentally observed ν_1 and ν_3 band profiles did however show excitation-dependent variations similar to those reported by Rives-Arnaud and Sheppard⁴ for *trans*-polyacetylene adsorbed on TiO₂. There was some similarity between the spectra observed for *trans*-(CH)_x on CsM and those reported for *trans*-polyacetylene produced on Al₂O₃,² alumina-supported rhodium,⁵ and Co(II) and Ni(II)-exchanged zeolite Y.⁶

As the excitation frequency increased, several distinct and quite systematic modifications of the band profile were observed. The ν_1 and ν_3 lines exhibited an almost

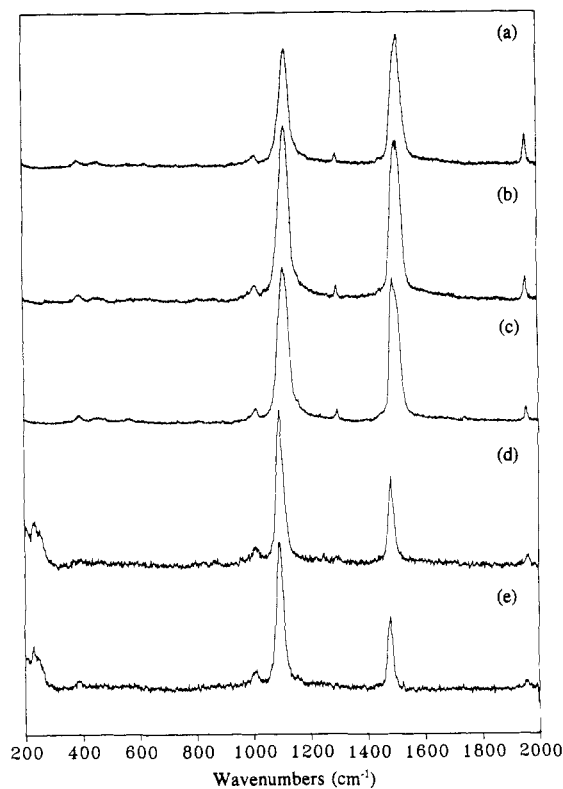


Figure 3. Raman spectrum of *trans*-(CH)_x on CsM in the region 200-2000 cm⁻¹. Excited at (a) 457.9, (b) 488.0, (c) 514.5, (d) 647.1, and (e) 676.4 nm.

symmetric band profile when excited at 457.9 and 514.5 nm. With 488.0-nm excitation, both lines had a prominent shoulder on the low-frequency edge. The fwhm of these bands was virtually constant having a value of ca 45 cm⁻¹ for these three cases (Table IV). Raman spectra recorded with red excitation (647.1 and 676.4 nm) showed a considerable reduction in the fwhm, decreasing to 17 (ν_1) and 26 cm⁻¹ (ν_3). These excitation-dependent variations in the band shape are interpreted as evidence that the *trans*-(CH)_x adsorbed on CsM consists of polymer molecules which are composed of segments having a range of conjugation lengths, these noninteracting segments being separated by structural defects of various types. This

Table II. Raman Band Positions Observed for the Fundamental Modes of *trans*-Polyacetylene Formed on Sodium (NaM) and Cesium (CsM) Mordenite Using Various Excitation Wavelengths

mordenite	excitation wavelength (nm)	ν_1 (cm ⁻¹)	ν_2 (cm ⁻¹)	ν_3 (cm ⁻¹)	ν_7 (cm ⁻¹)
NaM	514.5	1509	1292	1126	1010
CsM	457.9	1512	1295	1123	1011
	465.8	1509	1296	1122	1012
	472.7	1508	1293	1122	1013
	476.5	1506	1294	1121	1010
	488.0	1505	1295	1120	1011
	496.5	1504	1295	1117	1009
	501.5	1502	1293	1116	1011
	514.5	1497	1294	1110	1008
	514.5 ^a	1511	1294	1125	1011
	647.1	1482	1294	1090	1010
	676.4	1480	1296	1088	1009

^a After 5 months exposure to air.

conclusion is in agreement with those of several other groups who have reported Raman spectroscopic studies of *trans*-polyacetylene absorbed on various other zeolitic and oxide hosts.^{4,6}

It is shown below that the *trans*-(CH)_x formed on CsM has a distribution of conjugation lengths ranging from less than 6 to at least 30 double bonds. Furthermore, the distinct absence of any observable doublet band structure with a sharp, intense band as the low-frequency component which was virtually unchanged with variation in excitation energies in Raman spectra (i.e., as is observed for high-quality free-standing films of *trans*-(CH)_x), precludes explanation of the observed band dispersion anomalies in terms of the hot luminescence model proposed by Mele.³⁶ Additionally these data indicate that the *trans*-polyacetylene formed on CsM is not composed predominantly of very long ($N_{C=C} > 30$) lengths of conjugation as is seen in samples of bulk polyacetylene produced by the Shirakawa technique.³⁷ The observed excitation variations in the ν_1 and ν_3 Raman line profiles are readily explained in terms of this resonance behaviour of the different conjugation lengths present in *trans*-(CH)_x. The band is considered to be composed of a series of closely separated, strongly overlapping Raman lines (of comparable band width estimated to be ca. 20 cm⁻¹),¹¹ each corresponding to light inelastically scattered by segments having the same number of uninterrupted conjugated double bonds. The different segment lengths will be in various degrees of resonance with the incident excitation wavelength, and will thus contribute in varying amounts to the overall band shape. Since the frequency of the ν_1 and ν_3 modes are intimately related to the conjugation lengths, the position of the peak maximum for given excitation and the profile of the band will be dominated by the segments whose $\pi \rightarrow \pi^*$ transition maximum corresponds most closely to the energy of incident excitation. Contributions from other less-enhanced lengths will be included in the wings of the stronger bands. The relative populations of the different conjugation lengths will also affect the band shape; if there is a large population of a particular length then these chains will scatter (inelastically) more light at a given frequency, and thus even though they may not be fully in resonance they could contribute significantly to overall band intensity, possibly appearing as shoulders. A further very important factor that must also be considered is the

presence of polymer molecules with a range of conjugation lengths. These different lengths will have $\pi \rightarrow \pi^*$ transition energies that are very nearly equivalent for successive lengths,³⁸⁻⁴⁰ and hence light scattered inelastically from segments having a certain number of conjugated double bonds will still fall within the visible absorption band of other segment lengths, and thus will not reach the detector, i.e., reabsorption of the Raman scattering by the sample itself will occur. This self-absorption will have a large effect on the observed Raman intensity and band profiles.

Band Positions. The frequencies of the ν_1 and ν_3 modes of *trans*-(CH)_x were observed to show a strong dependence on the wavelength of the incident excitation, these bands shifting to lower frequencies as the frequency decreased. The ν_1 band shifted from 1510 to 1480 cm⁻¹ i.e., a ca. 30-cm⁻¹ shift to lower frequency as the excitation wavelength was changed from 457.9 to 676.4 nm. The ν_3 mode exhibited a decrease of similar magnitude, decreasing from 1123 cm⁻¹ when excited at 457.9 nm to 1088 cm⁻¹ when red 676.4-nm excitation was incident. These shifts can be seen in Figures 3 and 4.

The systematic nature of the ν_1 and ν_3 band position shifts is further illustrated in the graphs presented in Figure 5. From Figure 5b the almost linear decrease of the ν_3 frequency with increasing excitation wavelength can be seen. This mode exhibited a decrease of -39 cm⁻¹/eV. The ν_1 band however showed a distinctly nonlinear dependence, the rate of change decreasing from -40 cm⁻¹/eV at blue wavelength -22 cm⁻¹/eV with red excitation (see Figure 5a). Similar shifts of the ν_1 and ν_3 bands have been observed by Heavyside et al.³ in their Raman spectroscopic studies of *trans*-(CH)_x on γ -Al₂O₃. These authors reported a decrease in the frequencies of the polyene bands as the activation temperature was increased, which was attributed to polymer having longer conjugation when formed on alumina activated at higher temperatures.

These peak shifts can be readily interpreted if the *trans*-(CH)_x is assumed to consist of a distribution of molecules having a range of conjugation lengths. The segments of longer conjugation length (and thus lower ν_1 and ν_3 frequencies) will be in resonance with longer excitation wavelengths and will be the dominant contribution to overall band shape (and position), while other segments having shorter conjugation lengths will not be in resonance with the long excitation wavelengths, and will contribute to the high frequency edge of the bands.

With short excitation wavelengths, the scattering from segments having fewer uninterrupted conjugated double bonds will dominate the band shape and therefore the band maximum will be observed at higher frequency.

Estimation of Conjugation Length. Kuhn,³⁸ Kuhn,³⁹ and Dewar⁴⁰ proposed equations which relate the number of uninterrupted conjugated double bonds, $N_{C=C}$, to the wavelength at which the maximum visible absorption, λ_{max} occurs. However, because visible absorption spectra could not be obtained for the sample of CsM with adsorbed *trans*-(CH)_x these equations could not be utilised to estimate $N_{C=C}$ as other groups have done.² Therefore the conjugation length in *trans*-(CH)_x was estimated from the experimentally observed frequencies of the ν_1 and ν_3 modes

(36) Mele, E. J. *Solid State Commun.* 1982, 44, 827.

(37) Shirakawa, H.; Ikeda, S. *Polym. J.* 1971, 2, 231.

(38) Kuhn, W. *Helv. Chim. Acta* 1948, 31, 1780.

(39) Kuhn, H. *J. Chem. Phys.* 1949, 17, 1198.

(40) Dewar, M. J. S. *J. Chem. Soc.* 1952, 3544.

Table III. Raman Band Positions (cm⁻¹) Observed with Various Exciting Lines for Some Combinations and Overtones of the Fundamental Modes of *trans*-Polyacetylene Formed on Sodium (NaM) and Cesium (CsM) Mordenite

mordenite	excitation wavelength (nm)	$\nu_3 + \nu_7$	$2\nu_3$	$\nu_2 + \nu_3$	$\nu_1 + \nu_7$	$\nu_1 + \nu_3$	$\nu_1 + \nu_2$	$2\nu_1/\nu_3(\text{CH})^a$	
NaM	514.5	n.o.	2250	n.o.	n.o.	2633	n.o.	2922 ^b	
CsM	457.9	2127	2238	2394	2516	2624	2810	2962	3020
	488.0	2130	2225	2410	2506	2615	2795	2965	3008
	514.5	n.o.	2216	2406	2504	2604	2790	2960	3001
	514.5 ^c	n.o.	2248	2417	2520	2630	2799	2981	3017
	647.1	n.o.	2180	n.o.	2565	n.o.	n.o.	2928	2988 ^d

^a Fermi resonance. ^b Distinctly asymmetric band. ^c After 5 months exposure to air. ^d Bands not well separated; n.o. = not observed.

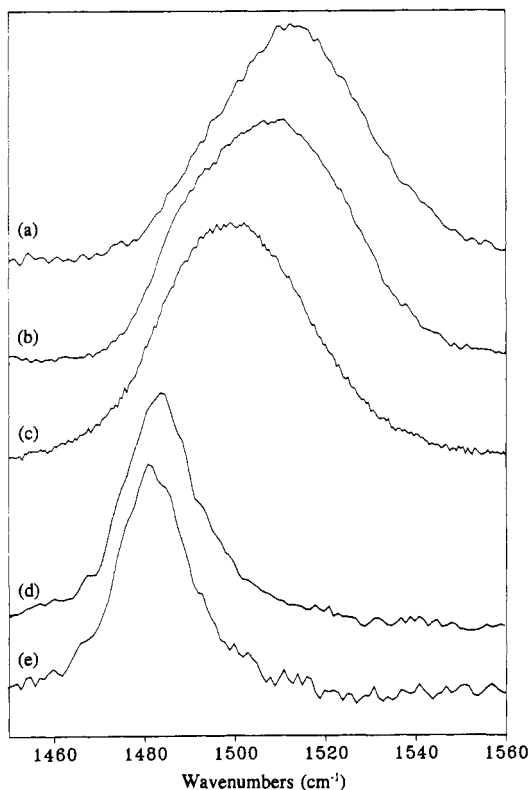


Figure 4. Variations observed in the Raman profile of the ν_1 band of *trans*-(CH)_x on CsM with different excitation wavelengths: (a) 457.9, (b) 488.0, (c) 514.5, (d) 647.1, and (e) 676.4 nm.

using the empirical relationships proposed by Harada et al.¹⁰ and Baruya et al.⁴¹ Using these relationships, $N_{\text{C}=\text{C}}$ values for *trans*-(CH)_x formed on CsM were obtained, after various periods of acetylene contact (see Table IV).

Effect of Exposure to Air. The effect of exposure of *trans*-(CH)_x adsorbed on CsM was studied because oxidative decomposition is one of the major problems preventing widespread application of polyacetylene as an electrically conducting medium.¹ Several changes were apparent in the Raman spectra recorded for samples exposed to air. It was observed that the positions of the ν_1 and ν_3 band maxima shifted slightly (ca. 0.5 cm⁻¹) to higher frequencies for consecutive spectra recorded of samples in direct contact with air during spectral acquisition. Such variations were not detected for samples held under vacuum after air exposure. Larger shifts were observed for samples which had been exposed to air for a period of time prior to recording the spectra. In these cases the magnitude of the shift increased with the period of the exposure of the sample to air. Listed in Table IV are the ν_1 and ν_3 band positions observed for *trans*-(CH)_x

on CsM after various periods of air contact. Also given in Table IV are the Raman shifts of these bands determined for the sample prior to exposure to air. Comparison of these frequencies also reveals that the rate at which the ν_1 and ν_3 bands shifted from their initial positions decreased markedly from 1 cm⁻¹/h during first few hours of exposure to only 0.005 cm⁻¹/h after 5 months of exposure when excited at 514.5 nm.

Typical Raman spectra obtained with 514.5-nm excitation for the ν_3 band over the region 1000–1250 cm⁻¹ after periods of air contact ranging from one day to five months may be seen in Figure 6b–e, respectively. Comparison with Figure 6a reveals not only the shift to higher frequencies but also the dramatic changes in the band shape.

Associated with these variations in band shapes were marked decreases in the band width, the full width at half-maximum (fwhm) being reduced from 44 to about 30 cm⁻¹. The observed band width was also dependent on the excitation wavelength. Similar but less pronounced variations in the shape and width of the ν_1 band were also observed. The largest band width reductions were observed in spectra recorded with the blue excitation (457.9 and 488.0 nm) which showed decreases of nearly 40% after 5 months of exposure to air.

These air-induced band shape modifications and fwhm reductions are very similar to those reported by Fitchen⁴² in his studies of effect of exposure of bulk *trans*-(CH)_x to air and are interpreted⁴³ as indicating the interruption of the conjugation within the longer segments to yield two or more segments having fewer uninterrupted conjugated double bonds. This probably occurs^{1,43} via an oxygen-induced reaction, possibly involving oxygen doping. Such a process is known to occur in free-standing films of *trans*-polyacetylene exposed to oxygen at room temperature.⁴³ The segments having fewer conjugated double bonds will be in resonance with shorter, rather than longer, excitation wavelengths and will therefore contribute to the observed shift of the band to higher frequencies (through both a reduction in the concentration of longer conjugated segments and an increase in the numbers of molecules having shorter lengths of conjugation).

Estimations of the number of uninterrupted conjugated double bonds ($N_{\text{C}=\text{C}}$) in the *trans*-(CH)_x formed on CsM after various periods of exposure to air are given in Table IV. A systematic decrease in the length of the segments of uninterrupted conjugated double bonds with increasing duration of air contact ($N_{\text{C}=\text{C}}$ values diminishing from about 27 prior to exposure, to less than 18 after 5 months in air) was observed, indicating a reduction in the quality

(42) Fitchen, D. B. *Mol. Cryst. Liq. Cryst.* 1982, 83, 95.

(43) Chien, J. C. W.; Wneck, G. E.; Karasz, F. E.; Warakowski, J. M.; Dickinson, L. C.; Heeger, A. J.; MacDiarmid, A. G. *Macromolecules* 1982, 15, 614.

(41) Baruya, A.; Gerrard, D. L.; Maddams, W. F. *Macromolecules* 1983, 16, 578.

Table IV. Observed Raman Frequencies, Full Bandwidths at Half-Maximum (fwhm), and Estimated^a Number of CC Double Bonds (N_{C-C}) for *trans*-Polyacetylene Formed on CsM That Had Been in Contact with Acetylene for 35 h and for the Same Sample after Various Periods of Exposure to Air

exposure period	exciting line/nm	ν_1 (cm ⁻¹)	fwhm (cm ⁻¹)	N_{C-C}		ν_3 (cm ⁻¹)	fwhm (cm ⁻¹)	N_{C-C} Harada
				Harada	Baruya			
unexposed	457.9	1510	46	12	14	1121	42	12
	488.0	1505	47	13	15	1116	44	14
	514.5	1493	45	18	19	1109	45	17
	647.1	1482	18	25	25	1092	27	27
	676.4	1480	17	27	26	1088	26	32
1 h	514.5	1495	45	17	19	1110	44	15
3 h	514.5	1496	46	16	19	1111	42	15
4 h	457.9	1512	45	12	14	1123	41	11
5 h	488.0	1504	47	13	16	1117	44	13
6 h	514.5	1497	44	16	18	1113	43	14
7 h	647.1	1485	17	23	23	1096	26	24
1 day	457.9	1513	43	11	13	1125	39	11
	488.0	1506	45	13	15	1117	42	13
	514.5	1498	41	16	18	1115	40	14
	647.1	1486	16	22	23	1097	25	23
7 days	457.9	1515	38	11	13	1127	35	10
	488.0	1512	43	12	14	1123	37	11
	514.5	1503	37	14	16	1118	38	13
	647.1	1490	15	19	21	1098	23	22
5 months	457.9	1520	29	10	12	1131	29	9
	488.0	1520	37	10	12	1129	34	10
	514.5	1511	36	12	14	1125	33	11
	647.1	1501	13	16	17	1105	20	18

^a N_{C-C} values calculated from the empirical relationships proposed by Harada and co-workers¹⁰ and Baruya *et al.*⁴¹

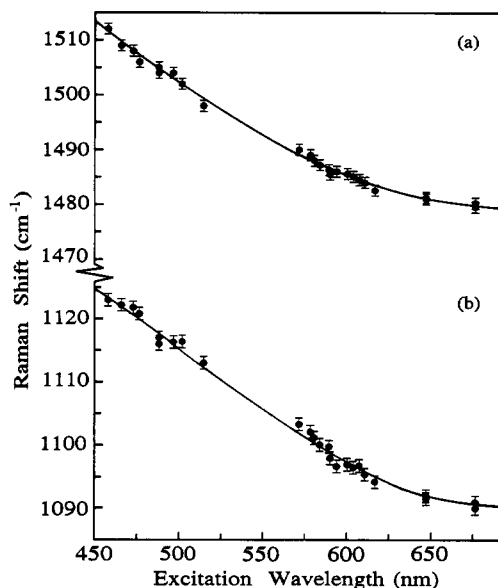


Figure 5. Raman shift of (a) the ν_1 and (b) the ν_3 bands of *trans*-(CH)_x on CsM observed with different excitation wavelengths.

of the *trans*-(CH)_x through exposure to air. This degradation was greatly accelerated by laser irradiation as evidenced by the increasing frequencies observed for the ν_1 and ν_3 modes between successive spectral acquisitions during which the sample was in direct contact with air. In the absence of oxygen, laser degradation of the polymer was not significant, as indicated by the reproducibility of the spectra after successive scans.

A decrease in the overall intensity (relative to the CsM 393 cm⁻¹ band) of the *trans*-(CH)_x Raman features was also observed with increasing period of exposure to air. This reduction in intensity, like the frequency shift discussed above, was to some extent dependent on the period of air exposure prior to obtaining the Raman spectra, but was greatly accelerated by laser irradiation.

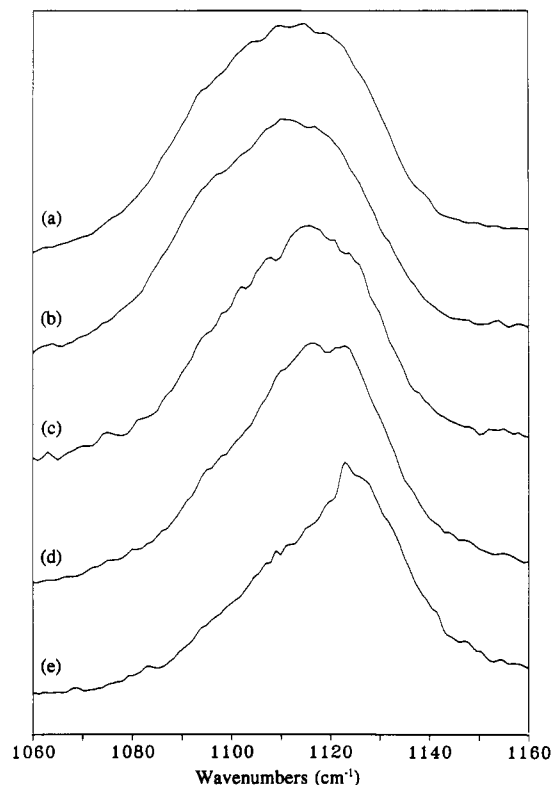


Figure 6. Variations observed in the Raman profile of the ν_3 band of *trans*-(CH)_x adsorbed on CsM (a) before air contact, and after exposure to air for (b) 1 day; (c) 2 days; (d) 7 days, and (e) 5 months. Excited at 514.5 nm, laser power 100 mW, resolution 2.7 cm⁻¹, sampling increment 0.5 cm⁻¹.

The intensity reduction was found to be dependent on both the period of laser irradiation and the laser flux incident on the sample. For instance, the Raman intensities of the ν_1 and ν_3 bands were reduced by nearly 60% during a 20-min period in which the sample was subjected to laser irradiation (514.5 nm, 180 mW) while exposed to air. Similarly, these intensities were reduced by almost

60% when the incident laser flux was doubled from 400 to 800 mW.

This reduction in intensity indicates that exposure to air also resulted in a considerable decrease in the total concentration of the *trans*-(CH)_x present on the CsM. Rives-Arnau and Sheppard⁴⁴ reported a drastic reduction in intensity of the *trans*-(CH)_x Raman features after admission of oxygen to the sample of polyacetylene adsorbed on TiO₂. They also noted the appearance of new features in the Raman spectra (in particular at ca. 1595, 1480, and 912 cm⁻¹, which they attributed to an aromatic *p*-polyphenyl species). However, no additional bands were detected in the Raman spectra recorded for *trans*-(CH)_x adsorbed on CsM after exposure of the samples to oxygen or air, which suggested that (CH)_x species were formed within the internal zeolite structure. This conclusion was supported by the evidence from a previous study⁴⁵ which detected monomeric reactant acetylene on internal channel sites of mordenite.

Excitation Profiles. To investigate whether the variation in the Raman ν_1 and ν_3 band profiles arises from a static inhomogeneous distribution of conjugation lengths within the *trans*-(CH)_x molecules on CsM or from other sources, sliced excitation profiles for these two modes were obtained. Intensities were measured at nine fixed frequencies (separated by 5-cm⁻¹ increments) within the ν_1 and ν_3 bands from Raman spectra recorded with nearly 40 different excitation wavelengths between 457.9 and 676.4 nm. These frequencies ranged from 1475 to 1515 cm⁻¹ and from 1085 to 1125 cm⁻¹ for the two modes, respectively. The observed intensities were corrected for instrument response and ν^4 dependence by using external calibration factors (based on the 992-cm⁻¹ line of liquid benzene) and also normalised for laser power effects by using the 393-cm⁻¹ line of mordenite. The corrected normalized intensities were then plotted versus excitation wavelength to give sliced excitation profiles, and the profiles for the ν_3 band are presented in Figure 7. Only five of the nine frequencies are shown, these best illustrating the inherent features.

The plots for both the ν_3 and ν_1 bands exhibit a single maximum per curve, with the position of the peak being dependent on the frequency; those for the highest frequency (1120 and 1510 cm⁻¹) peaking with incident photon energy of about 2.70 eV (ca. 455-nm wavelength excitation) and the lowest frequencies (1090 and 1480 cm⁻¹) reaching maxima near 1.95 eV (ca. 650 nm). The curves for the other frequencies within the ν_3 band (namely 1095, 1100, and 1115 cm⁻¹) exhibit maxima at excitation wavelengths of ca. 610, 590, and 510 nm, respectively (Figure 7), while the ν_1 frequencies 1490, 1495, and 1500 cm⁻¹ peaked with ca. 610-, 580-, and 520-nm excitation respectively.

These sliced excitation profiles display definite dispersive behavior, with enhanced scattering peaks apparent, the position of these maxima shifting progressively towards higher energies with increasing vibrational frequencies. These results are in good qualitative agreement with those reported for the ν_1 band of bulk *trans*-polyacetylene by Lichtmann et al.⁴⁶ They are however quite distinct from

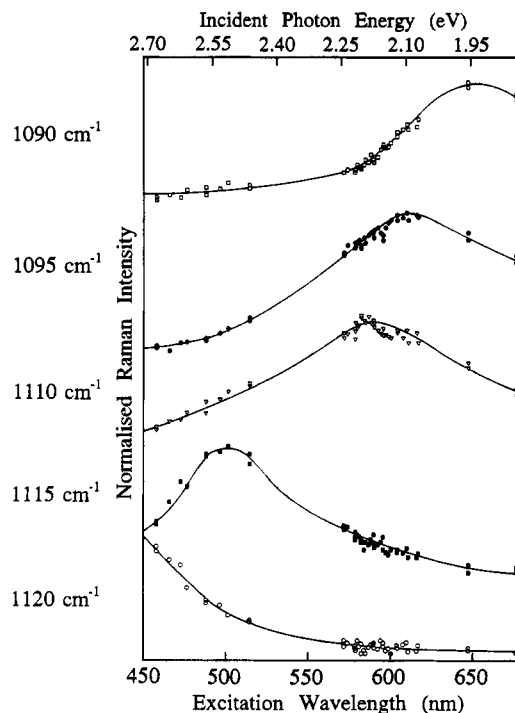


Figure 7. Sliced excitation profiles for the Raman intensity at five frequencies within the ν_3 band of *trans*-(CH)_x on CsM.

the sliced excitation profile of *trans*-(CH)_x reported by Lauchlan et al.⁴⁷

In agreement with Lichtmann et al.,⁴⁶ it was concluded that the sliced excitation profiles obtained for the ν_1 and ν_3 bands of *trans*-(CH)_x adsorbed on CsM indicated that the polymer was composed of molecules containing segments with a range of conjugation lengths. Furthermore the results show that the excitation dependence of the position and shape of these two bands are not independent of one another but are two interrelated phenomena, probably arising from the same cause. Although it is possible that the hot luminescence process may be a contributing factor in the observed band dispersion anomalies, it is not the major effect as Lauchlan et al.,⁴⁷ and Mele³⁶ proposed because the band shapes of *trans*-(CH)_x on CsM did not exhibit the doublet structure associated with that.

Hence the most plausible explanation for the observed excitation energy dependence of the profiles and positions of the Raman ν_1 and ν_3 bands is the presence of segments having a range of conjugation lengths, certain lengths coming into resonance with particular excitation wavelengths (i.e., when the $\pi \rightarrow \pi^*$ transition energies approach and coincide with that of the incident excitation) and thus dominating the observed band shape (and determining the position of the maximum). The other segment lengths will be in lesser degrees of resonance with the incident excitation, with the amount of resonance enhancement diminishing as the number of conjugated double bonds deviates further from those in the highest degree of resonance. The overall band profile is thus considered to be the result of the superposition of the lines for all the different conjugation lengths, the longer segments contributing to the low-frequency edge of the band, and the lines for the segments with fewer conjugated double bonds

(44) Rives-Arnau, V.; Sheppard, N. *J. Chem. Soc., Faraday Trans 1* 1981, 77, 953.

(45) Millar, G. J.; Lewis, A. R.; Bowmaker, G. A.; Cooney, R. P. *J. Mater. Chem.*, in press.

(46) Lichtmann, L.; Fitchen, D. B.; Temkin, H. *Synth. Met.* 1979, 1, 139.

(47) Lauchlan, L.; Chen, S. P.; Etemad, S.; Kletter, M.; Heeger, A. J.; MacDiarmid, A. G. *Phys. Rev. B* 1983, 27, 2301.

being seen in the high frequency tail of the band. The individual components are not resolved because of the very small frequency shifts observed between segments with consecutive numbers of double bonds.

Conclusions

It is concluded that the formation of *trans*-polyacetylene on cesium and sodium mordenite occurs predominantly within the main channels of the mordenite microcrystals. The restrictions of the channel size in mordenite limit the occupation of a channel to a single polymer molecule and this would preclude the possibility of cross-linking. Moreover, it seems likely that the *trans*-(CH)_x molecules formed obstruct the channels and prevent further diffusion of gaseous acetylene thereby limiting the yield and length of the polyacetylene formed. Oxygen molecules are however, small enough to travel along the occupied mordenite channels to cause irreversible degradation of the polymer molecules by interrupting the conjugation. The lower yields and shorter conjugation lengths produced on the NaM relative to CsM parallels the results of an earlier study of the polymerization of acetylene on alkali

metal ion exchanged faujasites.² Further work is required to elucidate the details of the mechanism of polymerization.

Exposure of *trans*-polyacetylene adsorbed on CsM to air or oxygen resulted in a reduction in the number of uninterrupted conjugated double bonds. Moreover, this degradation increased as the sample was left in contact with air for longer periods. Chain scission, reduction of conjugation length, formation of benzene or aromatic species are the prevalent processes which occur if *trans*-(CH)_x is subjected to high temperatures in the presence of oxygen. However, apart from the reduction in the conjugation length and loss of the polymer, none of the products associated with the other reactions were detected. Laser-induced heating of the sample in the presence of air caused rapid destruction of the *trans*-(CH)_x.

Acknowledgment. This work was supported by the University of Auckland Research Committee. G.J.M. acknowledges the award of a New Zealand Vice Chancellors' Committee postdoctoral fellowship.